Check for updates

ARTICLE

Perceived stress modulates the activity between the amygdala and the cortex

Inês Caetano [1,2,3], Sónia Ferreira[1,2,3], Ana Coelho[1,2,3], Liliana Amorim[1,2,3,4], Teresa Costa Castanho[1,2,3,4], Carlos Portugal-Nunes [1,2,3,5], José Miguel Soares[1,2,3], Nuno Gonçalves[1,2,3], Rui Sousa [1,2,3,6], Joana Reis[1,2,3], Catarina Lima[1,2,3], Paulo Marques[1,2,3], Pedro Silva Moreira[1,2,3], Ana João Rodrigues [1,2,3], Nadine Correia Santos [1,2,3], Pedro Morgado [1,2,3], Ricardo Magalhães[1,2,3], Maria Picó-Pérez [1,2,3], Joana Cabral [1,2,3] and Nuno Sousa [1,2,3,4 ✉]

The significant link between stress and psychiatric disorders has prompted research on stress's impact on the brain. Interestingly, previous studies on healthy subjects have demonstrated an association between perceived stress and amygdala volume, although the mechanisms by which perceived stress can affect brain function remain unknown. To better understand what this association entails at a functional level, herein, we explore the association of perceived stress, measured by the PSS10 questionnaire, with disseminated functional connectivity between brain areas. Using resting-state fMRI from 252 healthy subjects spanning a broad age range, we performed both a seed-based amygdala connectivity analysis (static connectivity, with spatial resolution but no temporal definition) and a whole-brain data-driven approach to detect altered patterns of phase interactions between brain areas (dynamic connectivity with spatiotemporal information). Results show that increased perceived stress is directly associated with increased amygdala connectivity with frontal cortical regions, which is driven by a reduced occurrence of an activity pattern where the signals in the amygdala and the hippocampus evolve in opposite directions with respect to the rest of the brain. Overall, these results not only reinforce the pathological effect of in-phase synchronicity between subcortical and cortical brain areas but also demonstrate the protective effect of counterbalanced (i.e., phase-shifted) activity between brain subsystems, which are otherwise missed with correlation-based functional connectivity analysis.

INTRODUCTION

Daily routines are getting increasingly stressful as modern society advances [1, 2]. Consequently, a new way of living, working, and interacting with others has emerged, with mental health concerns growing as a result of this transition [3, 4].

The way stress influences the brain has been examined at several levels, including molecular, cellular, and network levels [5–9]. Notwithstanding, it was the development of advanced neuroimaging techniques that potentiated our knowledge of brain morphology, connectivity, and function [6, 10–17]. Moreover, emergent algorithms for functional Magnetic Resonance Imaging (fMRI) data analysis have expanded the potential of neuroimaging studies to investigate the pathophysiology of brain disorders [15, 18–20]. Of relevance, whereas traditional static connectivity metrics tells us, on average, how synchronized two brain regions are (fine spatial resolution but no temporal definition), more recent functional dynamic analyses enable the identification of brain states resulting from spontaneous fluctuations of brain activity, thus providing spatiotemporal information (although with lower spatial definition) [21–23]. In particular, different clinical and pre-clinical psychiatric symptoms have

recently been associated with disrupted phase-locking patterns in fMRI signals between brain regions captured with Leading Eigenvector Dynamics Analysis (LEiDA) [24–26]. This reinforces the emerging hypothesis that optimal functional brain interactions may not necessarily be related to synchronized co-activation (as captured with static correlation-based analysis), but instead to delayed interactions leading to counterbalanced activations and de-activations between different brain subsystems [27–30].

It is well-established that chronic stress is a significant risk factor for the emergence of diseases such as post-traumatic stress disorder [31, 32], anxiety [33, 34], major depression disorder [33, 35], bipolar disorder [36, 37] and schizophrenia [38, 39]. However, due to the unique characteristics of each pathology, discovering how the brain is altered before disease onset is highly beneficial to the understanding of stress neurobiology and even crucial if considering mental preventive interventions [40–43].

Interestingly, when analyzing the relationship between perceived stress and brain morphology, a positive association between amygdala volume and perceived stress is observed [44, 45]. However, the way perceived stress affects brain function

[1]Life and Health Sciences Research Institute (ICVS), School of Medicine, University of Minho, 4710-057 Braga, Portugal. [2]ICVS/3B's, PT Government Associate Laboratory, 4710-057 Braga/Guimarães, Portugal. [3]Clinical Academic Center—Braga (2CA), 4710-243 Braga, Portugal. [4]Association P5 Digital Medical Center (ACMP5), 4710-057 Braga, Portugal. [5]CECAV —Veterinary and Animal Science Research Centre, Quinta de Prados, 5000-801 Vila Real, Portugal. [6]Departamento de Psiquiatria e Saúde Mental, Centro Hospitalar Tondela-Viseu, 3500-228 Viseu, Portugal. ✉email: njcsousa@med.uminho.pt

is still unclear, particularly if considering the small sample size of non-pathological studies in the literature [46–53].

Herein, we used a large cohort of resting-state fMRI data from healthy subjects of varying ages to gain a deeper insight into the impact of perceived stress on the functional interactions between brain areas. Based on the morphological results of our previous study [44], in which a positive association between the right amygdala volume and PSS10 scores was observed in a cohort oh young adults, we started by evaluating the association of perceived stress with amygdala seed-based connectivity (fine spatial resolution). Subsequently, we explored the disseminated effect of perceived stress on dynamic connectivity at a whole-brain level (spatiotemporal resolution). We hypothesized that differences in perceived stress would be reflected in amygdala connectivity, as well as in the expression of functional connectivity patterns involving emotional processing regions.

MATERIALS/SUBJECTS AND METHODS
Ethics statement
This study followed the criteria outlined in the Declaration of Helsinki (59th amendment) and was approved by the national and local ethics review board committees (*Comissão Nacional de Protecção de Dados*, *Comissão de Ética para a Saúde of Hospital de Braga*, and *Subcomissão de ética para as ciências da vida e da saúde* from University of Minho). All participants were informed about the study's goals and signed informed consent. Informed consent was also signed by the parents of participants under the age of 18.

Participants and study design
This work gathered 252 participants. Being a healthy individual and having the capability to undergo an MRI session were the primary inclusion criteria. Non-acceptance or inability to understand informed consent, individual choice to withdraw from the study, presence of any comorbidity from the central nervous system, or diagnosis of any neuropsychiatric illness were all exclusion criteria.

The protocol of this study consisted of a single evaluation. First, participants were characterized in terms of age, sex, and psychosocial stress. For the psychological assessment, participants were required to fill out the 10-items perceived stress scale (PSS10) questionnaire to quantify chronic psychosocial stress in the last month. After this, participants were submitted to an MRI session, performing an anatomical acquisition and a resting-state fMRI.

The anatomical images were used to preprocess fMRI data. The resting-state scans were used to explore the association of perceived stress with static and dynamic brain connectivity. For the static connectivity, a seed-based approach was followed. For the dynamic connectivity, a whole-brain data-driven analysis was conducted.

Participant characterization
Participants' demographic and psychological characterization was made using SPSS version 23 (IBM, SPSS, Chicago, IL, USA). Each variable was checked for normality, and non-parametric tests were applied where the assumption was not met. Sex factor was used in between-groups comparisons. A correlation between PSS10 scores and age was also made. The statistical significance was established for $a = 0.05$.

MRI data acquisition
The MRI acquisitions were made at the Hospital of Braga (Braga, Portugal), using a clinical approved Siemens Magnetom Avanto 1.5T MRI scanner (Siemens Medical Solutions, Erlangen, Germany), with a 12-channel receive-only head coil. After the acquisition, all images were examined by a licensed neuro-radiologist to ensure that the scans were not adversely influenced by head motion and

to confirm that participants did not have any pathologies or brain lesions.

Structural MRI. Anatomical acquisition consisted of one high-resolution T1-weighted Magnetization-Prepared Rapid Acquisition with Gradient Echo sequence (MPRAGE), with the following parameterization: voxel size $= 1 \times 1$ mm^2, slice thickness $= 1$ mm repetition time (TR) $= 2.73$ s, echo time (TE) $= 3.48$ ms, flip angle (FA) $= 7°$, field of view (FoV) $= 256$ mm, and 176 sagittal slices with no gap.

Resting-state functional MRI. Before the acquisition, participants were told to remain motionless with closed eyes, not to fall asleep, and not to think about anything specific. The fMRI acquisition consisted of a Blood Oxygenation Dependent Level (BOLD) sensitive echo-planar imaging, with the following parameterization: voxel size $= 3.5 \times 3.5$ mm^2, slice thickness $= 3.5$ mm, TR $= 2$ s, TE $= 30$ ms, FA $= 90°$, FoV $= 1344$ mm, 30 axial slices, slice gap $= 0.48$ mm, and 180 volumes.

MRI data preprocessing
Results included in this manuscript come from preprocessing performed using *fMRIPrep* 1.4.1 [19, 54] (RRID:SCR_016216), which is based on *Nipype* 1.2.0 [55, 56] (RRID:SCR_002502). A full description of the preprocessing pipeline can be found in the Supplementary material.

Amygdala seed-based connectivity
Seed-based connectivity analyses were performed using FSL (FMRIB Software Library, version 6.0, Analysis Group, FMRIB, UK) [57–59]. Firstly, the left and right amygdala masks were created using the Automated Anatomical Labeling (AAL) atlas [60, 61]. Herein, the mask of the right amygdala was centered in [32, 0, −30] (coordinates in mm) and composed of 248 voxels. With a voxel size of 220, the left amygdala mask was centered in [−24, −2, −28]. Then, the mean time series of each seed region were extracted for each participant and cross-correlated with all other brain voxels' time series. After this step, individual amygdala seed connectivity maps were considered the variable of interest, perceived stress (measured by PSS10 scores) as the independent term, and age and sex as covariates. Notably, due to the differences in magnitudes, PSS10 scores, age and sex covariates were standardized prior to statistical analysis. Finally, the association with perceived stress was estimated using the FSL *randomize* function, a non-parametric permutation method, considering 5000 permutations with statistical significance $a = 0.05$ after threshold-free cluster enhancement (TFCE) and family-wise error rate (FWE-R) correction [62]. The statistically significant clusters obtained were labeled with the AAL2 [60], and the BrainNet Viewer software was used for the visualization of results [63].

In order to further explore the results obtained with the right and left seed-based analysis for the total sample, two additional analysis were conducted: a left seed-based connectivity association with PSS10 scores in the total sample with a less restrictive threshold for statistical significance (setting $α = 0.1$); and a right seed-based connectivity association with PSS10 scores in individual subgroups of younger (15–25 years) and older adults (75–85 years).

Dynamic functional connectivity
The dynamic functional connectivity analysis was performed using the LEiDA method, which captures recurrent patterns of phase-locking between brain areas [18, 64]. Importantly, it allows estimating the probability of occurrence of each phase-locking pattern in each fMRI scan, providing a quantitative measure to compare with perceived stress (measured by PSS10 scores).

The mean fMRI signal for each of the $N = 94$ non-cerebellar brain regions of the AAL2 atlas was extracted for each subject, and the signal phase was computed using the Hilbert transform. After removing the first and last time points, at each of the $T = 178$ time points, an instantaneous $N \times N$ functional connectivity matrix was computed as the cosine of the phase difference between each pair of brain regions, and the $1 \times N$ leading eigenvector (i.e., associated with the largest magnitude eigenvalue) was saved for each timepoint, generating an $N \times T$ matrix capturing the dominant pattern of phase interactions for each timepoint.

Previous works have shown that these patterns can be clustered into a reduced set of phase-locking patterns, where the subsets of brain areas shifting in phase from the rest of the brain reveal known resting-state networks from the literature [64, 65]. Since the number of patterns defined is not a fixed number and only affects the sensitivity of the method, we ran the algorithm from $k = 2$ to $k = 20$, with k representing the number of patterns to cluster the data into (using the cosine distance and 500 iterations per k). For each of the 252 participants s, the probability of occurrence P(s,c,k) was calculated for each pattern c obtained for each k (with $c = 1,...,k$). For the statistical analysis, we used a partial correlation to measure the association between each pattern probability and PSS10 scores while controlling for age and sex factors. Notably, the significance was established for $a = 0.05$, and the obtained p values were corrected for the number of clusters tested (e.g., for $k = 16$, considering 16 independent multiple comparisons, the p value was divided by 16).

RESULTS

Cohort characterization

The participants' socio-demographic, psychological, and volumetric brain characterization (left and right amygdala, total GM, and eTIV) are presented in Table 1. In addition, the raw PSS10 scores, as well as the descriptive statistics of all cortical and subcortical regions can be consulted in Supplementary Fig. 1 and Supplementary Table 1, respectively.

A Mann–Whitney U test indicated that no age differences were found between males and females ($U = 6940.5$, $p = 0.136$).

An independent sample t-test indicated higher perceived stress scores in females than in males ($t (250) = -2.212$, $p = 0.028$, $d = 0.28$). A negative association between PSS10 scores and age was also found ($r (252) = -0.226$, $p < 0.001$).

Regarding brain volumes, both total GM and eTIV were significantly higher for males than females ($U = 5491$, $p < 0.001$, $r = 0.25$; and $t (250) = 9.691$, $p < 0.001$, $d = 1.25$ respectively).

Static seed-based connectivity

A positive association between PSS10 scores and right amygdala seed-based connectivity was observed within 17 clusters. As illustrated in Fig. 1, the cluster with the highest connectivity strength is peaked in the right Superior Frontal Gyrus (SFG) (cluster 1), also embracing part of the right Middle Frontal Gyrus (MFG). A cluster centered in the right MFG (2) and another in the right SFG (3) revealed almost the same strength of association. Interestingly, the next cluster presenting enhanced connectivity is on the right superior parietal lobule, specifically on the right precuneus (4). Next, centered in the MFG, cluster number 5 is the only one placed entirely on the left hemisphere. We also found clusters peaked in the anterior and middle right cingulate (clusters 7 and 14). Importantly, we observed that several other clusters of the SFG and MFG tend to synchronize with the right amygdala when perceived stress is increased (clusters 8, 10, 12 in SFG and clusters 9 and 15 [only 4 voxels] in the MFG). Importantly, cluster 10 (SFG) and cluster 9 (MFG), although with considerable voxel size (313 and 188, respectively), did not reveal heightened association with the right amygdala seed-region, particularly when compared to other clusters with smaller sample sizes.

Table 1. Demographic and psychological characterization of participants.

	Demographic		Psychological	Brain volume (mm³)			
	N (%)	Age (years)	Perceived stress (PSS10)	Right amygdala	Left amygdala	Total GM	eTIV
Global population	252 (100%)						
Min		15	1	9.46×10^2	8.50×10^2	4.39×10^5	1.14×10^6
Max		84	34	2.62×10^3	2.14×10^3	8.35×10^5	1.99×10^6
Mean ± SD		39.2 ± 21.20	15.4 ± 6.82	$1.43 \times 10^3 \pm 2.21 \times 10^2$	$1.35 \times 10^3 \pm 2.10 \times 10^2$	$6.27 \times 10^5 \pm 7.77 \times 10^4$	$1.56 \times 10^6 \pm 1.65 \times 10^5$
Male	109 (43.3%)						
Min		15	2	1.04×10^3	1.01×10^3	5.05×10^5	1.24×10^6
Max		80	29	2.62×10^3	2.14×10^3	8.35×10^5	1.99×10^6
Mean ± SD		42.6 ± 21.72	14.3 ± 6.44	$1.55 \times 10^3 \pm 2.42 \times 10^2$	$1.45 \times 10^3 \pm 2.08 \times 10^2$	$6.53 \times 10^5 \pm 8.25 \times 10^4$	$1.66 \times 10^6 \pm 1.58 \times 10^5$
Female	143 (56.7%)						
Min		15	1	9.46×10^2	8.50×10^2	4.39×10^5	1.14×10^6
Max		84	34	1.73×10^3	1.69×10^3	7.37×10^5	1.80×10^6
Mean ± SD		36.7 ± 20.51	16.3 ± 7.00	$1.35 \times 10^3 \pm 1.57 \times 10^2$	$1.28 \times 10^3 \pm 1.76 \times 10^2$	$6.07 \times 10^5 \pm 6.76 \times 10^4$	$1.49 \times 10^6 \pm 1.23 \times 10^5$

Demographic, psychological and brain morphometry characterization of the population included in this study.
eTIV Estimated Intracranial Volume, GM Gray matter, SD Standard Deviation.

Fig. 1 Results from the static connectivity: Positive association of right amygdala seed-based connectivity with PSS10 scores. A positive association between PSS10 scores and right amygdala seed-based connectivity was observed within 17 clusters. **A** *Representation of the most significant clusters obtained*. Each voxel is colored by its statistical significance, and the right amygdala seed region is colored in blue. **B** *3D representation of all clusters obtained, as well as its connection with right amygdala*. Each cluster is represented by a sphere colored by the strength of the connectivity (stronger connection in yellow). Spheres sizes were defined as an approximation of clusters sizes, using a pre-defined range interval. Seed-Based connectivity analysis were made using FSL, with individual seed connectivity maps as the variable of interest, PSS10 scores as the independent term, and age and sex as covariates. The statistical significance was considered for p values < 0.05, after threshold-free cluster enhancement (TFCE) and family-wise error rate (FWE-R) correction.

Clusters 6 and 11 are peaked in the Inferior Frontal Gyrus (IFG), on the pars opercularis and pars triangularis, respectively. Finally, with the most negligible strength of association and lowest voxel size, clusters 16 (6 voxels) and 17 (2 voxels) are also centered in the IFG (pars triangularis and pars orbitalis). A more detailed description of all the clusters in which connectivity with the right amygdala is positively associated with stress is presented in Table 2.

When exploring the positive association between PSS10 scores and left amygdala seed-based connectivity, no significant results were found (for the statistical significance of $a = 0.05$). However, as a way of further explore a possible tendency of association, we decided to lower the threshold for statistical from $a = 0.05$ to $a = 0.1$, as previously described in the methods section. With this new (and less restrictive) threshold, we found a cluster peaked in the right SFG ($x = 24$, $y = 56$, $z = 14$, in mm; cluster size = 36; peak p value = 0.065 and cluster mean p value = 0.07). Interestingly, this cluster overlaps with cluster number 1 reported above (Fig. 1),

which has been shown to have the highest connectivity strength with the right amygdala. A visual representation of these results is presented in Supplementary Fig. 2.

When conducting the individual subgroup analysis (younger and older adults), although with a smaller number of subjects per decade, the data shows that the right amygdala connectivity positively associates with PSS in both younger and older cohorts. Interestingly, this association was slightly different among age groups: whereas in younger subjects major clusters embrace precuneus, cingulate gyrus, frontal pole, frontal orbital cortex, lateral occipital cortex, paracingulate gyrus, and middle frontal gyrus; in older subjects we found positive associations with PSS mainly in postcentral, precentral, middle frontal and temporal gyrus and, importantly, a positive association of the right amygdala with contralateral subcortical structures (i.e., left putamen, hippocampus and amygdala). No other significant associations between amygdala connectivity and PSS were found (see Supplementary Fig. 3 for details).

Table 2. Clusters resulting from the regression analysis between the right amygdala seed-based connectivity and PSS10 scores.

Cluster Index	Cluster size	Peak					AAL2 description	Brain region label
		t value	*p* value[a]	MNI coordinates (*mm*)				
				x	*y*	*z*		
1	257	4.643	0.016	42	62	−4	67% (4) Frontal Sup 2 R 33% (6) Frontal Mid 2 R	SFG (dorsolateral) R MFG R
2	98	4.471	0.016	48	24	38	92% (6) Frontal Mid 2 R 8% (10) Frontal Inf Tri R	MFG R IFG (triangular part) R
3	36	4.417	0.025	24	36	20	71% (4) Frontal Sup 2 R 29% (6) Frontal Mid 2 R	SFG (dorsolateral) R MFG R
4	97	4.027	0.025	10	−70	28	87% (72) Precuneus R 11% (38) Cingulate Mid R	Precuneus R Middle Cingulate & Paracingulate Gyri R
5	22	3.932	0.043	−26	50	8	70% (5) Frontal Mid 2 L 30% (3) Frontal Sup 2 L	MFG L SFG (dorsolateral) L
6	42	3.891	0.030	48	16	14	100% (8) Frontal Inf Oper R	IFG (opercular part) R
7	20	3.861	0.041	14	44	2	45% (36 Cingulate Ant R 40% (22) Frontal Med Orb R 15% (20) Frontal Sup Medial R	Anterior Cingulate & Paracingulate Gyri R SFG (medial orbital) R SFG (medial) R
8	26	3.800	0.042	16	20	46	100% (4) Frontal Sup 2 R	SFG (dorsolateral) R
9	188	3.791	0.023	32	14	48	99% (6) Frontal Mid 2 R	MFG R
10	313	3.787	0.018	−2	32	38	73% (19) Frontal Sup Medial L 21% (20) Frontal Sup Medial R	SFG (medial) L SFG (medial) R
11	18	3.750	0.038	58	24	2	100% (10) Frontal Inf Tri R	IFG (triangular part) R
12	11	3.706	0.046	−2	22	42	82% (19) Frontal Sup Medial L 18% (15) Supp Motor Area L	SFG (medial) L Supplementary Motor Area L
13	36	3.686	0.032	42	28	−22	81% (30) OFCpost R 11% (32) OFClat R 8% (28) OFCant R	POG R LOG R AOG R
14	8	3.513	0.048	6	18	44	50% (38) Cingulate Mid R 50% (20) Frontal Sup Medial R	Middle cingulate & paracingulate gyri R SFG (medial) R
15	4	3.289	0.048	34	22	60	100% (6) Frontal Mid 2 R	MFG R
16	6	3.031	0.048	44	46	−4	50% (12) Frontal Inf Orb 2 R 33% (10) Frontal Inf Tri R 17% (6) Frontal Mid 2 R	IFG (pars orbitalis) R IFG (triangular part) R MFG R
17	2	2.815	0.050	52	28	28	100% (10) Frontal Inf Tri R	IFG (triangular part) R

A positive association between perceived stress scores and amygdala connectivity was observed in 17 clusters.
The seed-based connectivity analysis was performed using FSL. The individual maps of the seed (right amygdala) connectivity were used as the variable of interest, PSS10 as the independent term, and age and sex as covariates. Due to the differences in magnitudes, all the variables were standardized prior to analysis. The association was estimated using the FSL *randomize* function, considering 5000 permutations and $a = 0.05$ after threshold-free cluster enhancement (TFCE) and family-wise error rate (FWE-R) correction. The results are presented by order of significance and the brain regions were labeled according to the automated anatomical atlas 2 (AAL2).
SFG Superior Frontal Gyrus, *MFG* Middle Frontal Gyrus, *IFG* Inferior Frontal Gyrus, *POG* Posterior Orbital Gyrus, *LOG* Lateral Orbital Gyrus, *AOG* Anterior Orbital Gyrus.
[a]With TFCE and) FWE-R correction at a significance level of 0.05.

No other significant associations between seed-based amygdala connectivity and PSS10 scores were found, including negative associations in both right and left hemispheres.

Dynamic functional connectivity
The LEiDA analysis revealed a particular pattern of phase-locking between brain areas whose probability of occurrence was
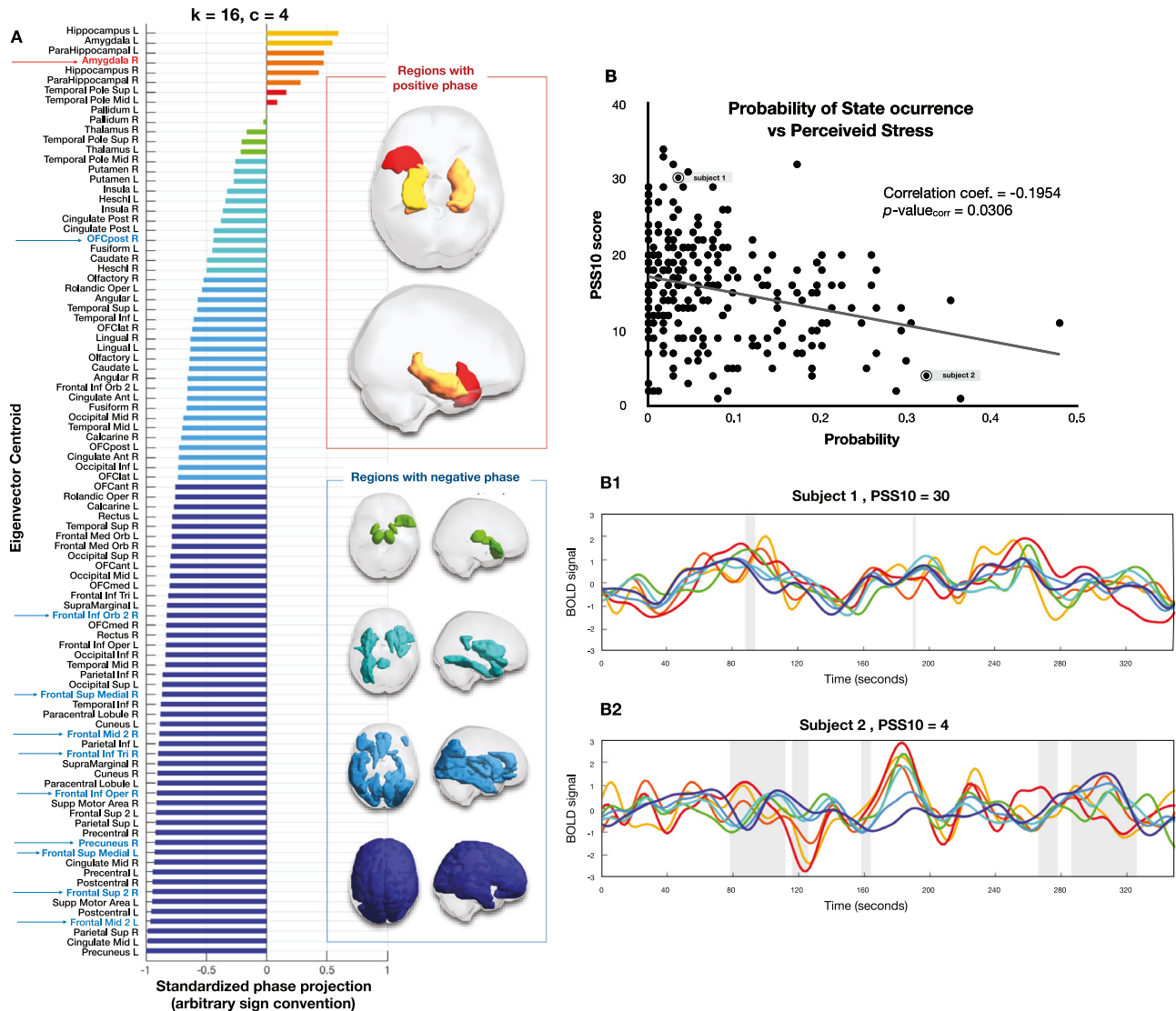
Fig. 2 Lower perceived stress relates to more counterbalanced activity between amygdala-hippocampus and the rest of the brain. A The functional phase-locking pattern represented by the cluster centroid V_c obtained for k = 16, c = 4. Elements in V_c(n) are sorted in descending order and colored (from orange to dark blue) according to their relative phase shift. The arrows on the left indicate the seed region (red) and the significant clusters (blue) from the seed-based analysis. On the right, a 3D rendering of the brain regions color-coded according to V_c(n). **B** The probability of occurrence of this pattern is plotted against PSS10 scores for all 252 subjects, as well as the trendline of the negative association found. **B1–B2** For two representative subjects, the BOLD signals averaged across subsystems with the same color in (**A**). The gray patches in the background highlight the time points when this pattern was detected, revealing clearly more occurrence for the subject with lower perceived stress. Notably, even when this pattern is not detected, there is clearly less synchronicity between the fMRI signals in subject 2.

negatively associated with PSS10 scores (detected for a partition into K = 16 clusters, cluster c = 4, with p_{corr} = 0.0306 corrected for the number of independent patterns compared and controlled for age and sex). Interestingly, the same functional subsystem obtained with K = 19, C = 4 also survived statistical correction (see Supplementary Fig. 4 for details about all states found and Supplementary Table 2 for all the p values and correlation coefficients).

As shown in Fig. 2A, this pattern is characterized by a phase shift in the fMRI signals of the bilateral hippocampus, amygdala, parahippocampal gyri, and the left superior and middle temporal pole. We note that the sign of phase projections is arbitrary and that the vector is bidirectional, meaning simply that when this pattern occurs, the brain areas with a given sign increase their fMRI signal, while the areas with opposite sign decrease their fMRI signal, or vice-versa.

This pattern of activity where the amygdala and hippocampus are in anti-phase with the rest of the brain was found to occur significantly more often in participants with lower perceived stress (Fig. 2B). Conversely, participants with high stress scores expressed this pattern less often. Interestingly, these results not only align but also provide insights into the findings from the seed-based analysis. Indeed, in the LEiDA analysis, the pattern occurring less often in participants with higher perceived stress is a pattern where the right amygdala (red arrow in Fig. 2A) is strongly phase-shifted with respect to the areas in blue.

For easy understanding of the association found (i.e., higher occurrence of the pattern in less stressed subjects), two arbitrary subjects with high and low PSS10 scores were, respectively, represented in subfigure B1 (Subject 1 with PSS10 = 30) and subfigure B2 (Subject 2 with PSS10 = 4) of Fig. 2. By focusing on the gray patches (which identify the periods of state occurrence),

we observed that the significant state was less dominant in stressed Subject 1 (only 2 small periods) than in the non-stressed Subject 2 (in which it occurred five times and in more extended periods). In addition, when looking at the BOLD signals, a higher synchronization is observed in stressed Subject 1 than in non-stressed Subject 2. Interestingly, desynchronization is particularly noticed during the periods of state occurrence. These differences are enhanced when looking to the right amygdala (represented in the red line) and comparing it to the majority of the seed-based regions (dark blue line).

DISCUSSION
In the present study, we used a sizeable cohort of healthy subjects of several ages to explore the interaction of perceived stress with the brain's static and dynamic connectivity. Static connectivity results show that increases in perceived stress are associated with stronger right amygdala connectivity with several frontal cortical nodes. On the other hand, the dynamic analysis revealed the existence of a functional state involving the amygdala and hippocampi, in which the probability of occurrence was found to negatively associate with PSS10 scores.

The hypothesis that PSS10 scores are associated with right amygdala connectivity was verified mainly in the right prefrontal cortex, right precuneus, and right anterior and middle cingulate. In addition, although not achieving statistical significance, a tendency of increased connectivity between the left amygdala and the right PFC was also observed. These results confirm the relevance of the pattern of connectivity between the amygdala and frontal cortical regions when processing emotional stimuli. Interestingly, this association between subjective psychological state and prefrontal-amygdala connectivity has been observed in previous work [66].

Curiously, our data also highlight the relevance of distinct patterns of brain hemispheric connectivity in the stress response, as suggested by previous literature. Indeed, a previous study has shown that the right PFC activity is associated with increased emotionality (positively associating with amygdala activity), whereas the left PFC relates with the downregulation of negative emotions (negatively associating with amygdala activity) [67]. Another study reveals that increases in self-reported sleep were negatively associated with distress severity and right amygdala-prefrontal FC, whereas no significant results were observed on the left hemisphere [66]. Importantly, although this work focusses on the effects of perceived stress independently of the subjects' sex and age, sex-related functional amygdala asymmetries were also observed in distinct Cahill's works [68–70]. For instance, when compared to woman, higher right amygdala functional connectivity was observed in man; contrasting to the greater left functional connectivity observed in women (when compared to man), in resting-state analysis [69]. Indeed, these conclusions may help unraveling our results, once they suggest that functional amygdala lateralization is not solely caused by the emotional input, but also respects both sex and hemispheric characteristics. Moreover, in a meta-analysis on brain activity in response to stress, the bias toward right hemisphere activation is also noticed, particularly in the right superior temporal gyrus and IFG [11]. Therefore, our data seems to capture the contrast between the right hemisphere's dominance on stress regulation and emotional processing, contrasting to the left hemisphere's prominence on linguistic and motor functions [71].

Our findings contrast with a previous work with a smaller sample size, in which the right amygdala-ventromedial prefrontal cortex FC was negatively related to stress in young adults, without significant correlations being observed in adults [53]. Notably, this contrast is even more highlighted when considering the individual analysis in a subgroup of young adults, in which a positive, but not any negative, association, was observed. Interestingly, by

conducting individual narrow aged analysis, it was demonstrated that perceived stress and amygdala connectivity are positively linked in both age groups (albeit with different nodes and with a very interesting subcortical lateralization in the case of the older ones). Furthermore, inconsistencies are emphasized by another study in which stronger resting-state connectivity between the left, and not the right, amygdala and (bilateral) regions such as the MFG, anterior cingulate and thalamus, is observed in subjects with higher levels of discrimination [72].

From a higher-level perspective, our seed-based results show alterations in the fronto-parietal network, which is known to be involved in several regulation processes [73, 74]. Most importantly, changes in fronto-limbic and fronto-parietal circuits have been linked to numerous stress-related psychopathologies [29, 73–77]. Indeed, rather than hamper specific individual brain regions' mechanisms, stress affects the connectivity within brain circuits causing a global impact at the neuromatrix [17]. Importantly, to confirm the stress repercussions at the network level, the study of dynamic connectivity is of value.

Using LEiDA, besides the identification of the most dominant brain states, it is possible to distinguish which patterns (or states) associate with variables of interest [18, 78]. Herein, our results show that increases in perceived stress are negatively associated with the occurrence of a functional state in which subcortical regions, including the amygdala and hippocampus, are shifted from the other regions of the brain, with the most significant shifts being observed in PFC regions.

A previous study on clinically stressed subjects demonstrated differential dynamic activation of right frontal areas, relating it to a PFC dysfunction and, consequently, to a diminished ability to downregulate amygdala activity [79]. Using a combination of static and dynamic techniques, another research highlighted the activity of frontal and parietal regions as biomarkers of negative stress [80].

By combining static with dynamic connectivity results, we have shown that the increase of perceived stress matches an increase in amygdala connectivity, alongside a reduction in the occurrence of the amygdala anti-phase state. Importantly, it is during this anti-phase state that major desynchronization in healthy subjects is observed. Indeed, denoting that state transitions seem to occur in periods of intermediate synchronization or desynchronization (not in the extremes), our results follow previous evidences supporting the critical brain hypothesis [81]. In short, criticality claims that neurons networks operate close to a critical point, easily crossing to a state in which the activity gradually increases, or to a phase in which the activity rapidly fades away [82]. Notably, several processing functions are optimized at this critical point, with the ability of the brain to be critical (and therefore shifting across phases) considered fundamental on healthy subjects [82]. Indeed, our results show that stressed subjects have increased amygdala hypersynchrony and reduced ability to shift across brain states (with fewer occurrences of the significant pattern), contrarily to non-stress individuals which are characterized by intermediate periods of synchrony and desynchrony of brain function, as for their higher ability to shift across brain states.

This study has limitations. Its cross-sectional, rather than longitudinal, design is one of the most significant drawbacks of our research. However, if on one side we cannot infer any causality regarding brain dynamics and perceived stress associations (limitation), on the other hand we were able to identify characteristics of a stressed brain that persist across the lifespan (advantage). Notably, in this work, we did not control for subjects' handedness. Assuming this as a limitation, we expect to include this control variable in future studies as we recognize the benefits of controlling for subjects' handedness in the further dissection of the functional asymmetries observed. The dynamic data-driven analysis (LEiDA) is still quite novel and, in the present study, confined to a non-clinical cohort. In light of these issues, future

research should focus on expanding the current observations to broader cohorts and in a longitudinal perspective.

In the present study, we explored the relationship between perceived stress and brain connectivity in a large cohort of healthy subjects with a broad age range. Our data reveal that increases in perceived stress were associated with altered patterns of both static and dynamic amygdala connectivity with frontal cortical regions. More specifically, we show that increased perceived stress is directly associated with increased amygdala connectivity with frontal cortical regions, which is driven by a reduced occurrence of an activity pattern where the signals in the amygdala and the hippocampus evolve in opposite directions with respect to the rest of the brain. In summary, these results reinforce the detrimental effect of in-phase synchronicity between subcortical and cortical brain areas but also demonstrate the protective effect of counterbalanced activity between brain subsystems.

DATA AVAILABILITY
The data that support the findings of this study are available from the corresponding author upon reasonable request.

CODE AVAILABILITY
FSL software is available by the authors at https://fsl.fmrib.ox.ac.uk/fsl/fslwiki/FslInstallation and LEiDA scripts at GitHub (https://github.com/juanitacabral/LEiDA).

REFERENCES
1. Fett A-KJ, Lemmers-Jansen ILJ, Krabbendam L. Psychosis and urbanicity: a review of the recent literature from epidemiology to neurourbanism. Curr Opin Psychiatry. 2019;32:232–41.
2. Gong Y, Palmer S, Gallacher J, Marsden T, Fone D. A systematic review of the relationship between objective measurements of the urban environment and psychological distress. Environ Int. 2016;96:48–57.
3. Lederbogen F, Ulshoefer E, Peifer A, Fehlner P, Bilek E, Streit F, et al. No association between cardiometabolic risk and neural reactivity to acute psychosocial stress. NeuroImage-Clin. 2018;20:1115–22.
4. Ritchie H, Roser M. Urbanization. Our World in Data. 2018.
5. Cerqueira JJ, Mailliet F, Almeida OFX, Jay TM, Sousa N. The Prefrontal Cortex as a Key Target of the Maladaptive Response to Stress. J Neurosci. 2007;27:2781–7.
6. Magalhães R, Barrière DA, Novais A, Marques F, Marques P, Cerqueira J, et al. The dynamics of stress: a longitudinal MRI study of rat brain structure and connectome. Mol Psychiatry. 2018;23:1998–2006.
7. Popoli M, Yan Z, McEwen BS, Sanacora G. The stressed synapse: the impact of stress and glucocorticoids on glutamate transmission. Nat Rev Neurosci. 2012;13:22–37.
8. Sousa N, Lukoyanov NV, Madeira MD, Almeida OFX, Paula-Barbosa MM. Reorganization of the morphology of hippocampal neurites and synapses after stress-induced damage correlates with behavioral improvement. Neuroscience 2000;97:253–66.
9. Yuen EY, Wei J, Liu W, Zhong P, Li X, Yan Z. Repeated Stress Causes Cognitive Impairment by Suppressing Glutamate Receptor Expression and Function in Prefrontal Cortex. Neuron 2012;73:962–77.
10. Koenig JI, Walker C-D, Romeo RD, Lupien SJ. Effects of stress across the lifespan. Stress 2011;14:475–80.
11. Kogler L, Müller VI, Chang A, Eickhoff SB, Fox PT, Gur RC, et al. Psychosocial versus physiological stress—Meta-analyses on deactivations and activations of the neural correlates of stress reactions. NeuroImage 2015;119:235–51.
12. Lucassen PJ, Pruessner J, Sousa N, Almeida OFX, Van Dam AM, Rajkowska G, et al. Neuropathology of stress. Acta Neuropathol. 2014;127:109–35.
13. Magalhães R, Novais A, Barrière DA, Marques P, Marques F, Sousa JC, et al. A Resting-State Functional MR Imaging and Spectroscopy Study of the Dorsal Hippocampus in the Chronic Unpredictable Stress Rat Model. J Neurosci. 2019;39:3640–50.
14. Novais A, Monteiro S, Roque S, Correia-Neves M, Sousa N. How age, sex and genotype shape the stress response. Neurobiol Stress. 2017;6:44–56.
15. Soares JM, Magalhães R, Moreira PS, Sousa A, Ganz E, Sampaio A, et al. A Hitchhiker's Guide to Functional Magnetic Resonance Imaging. Front Neurosci. 2016;10.
16. Soares JM, Marques P, Alves V, Sousa N. A hitchhiker's guide to diffusion tensor imaging. Front Neurosci. 2013;7.
17. Sousa N. The dynamics of the stress neuromatrix. Mol Psychiatry. 2016;21:302–12.
18. Cabral J, Vidaurre D, Marques P, Magalhães R, Silva Moreira P, Miguel Soares J, et al. Cognitive performance in healthy older adults relates to spontaneous switching between states of functional connectivity during rest. Sci Rep. 2017;7:5135.
19. Esteban O, Markiewicz CJ, Blair RW, Moodie CA, Isik AI, Erramuzpe A, et al. fMRIPrep: a robust preprocessing pipeline for functional MRI. Nat Methods. 2018;16:111–6.
20. Lv H, Wang Z, Tong E, Williams LM, Zaharchuk G, Zeineh M, et al. Resting-State Functional MRI: Everything That Nonexperts Have Always Wanted to Know. Am J Neuroradiol. 2018;39:1390–9.
21. Bassett DS, Sporns O. Network neuroscience. Nat Neurosci. 2017;20:353–64.
22. Biswal B, Zerrin Yetkin F, Haughton VM, Hyde JS. Functional connectivity in the motor cortex of resting human brain using echo-planar mri. Magn Reson Med. 1995;34:537–41.
23. Menon SS, Krishnamurthy K. A Comparison of Static and Dynamic Functional Connectivities for Identifying Subjects and Biological Sex Using Intrinsic Individual Brain Connectivity. Sci Rep. 2019;9:5729.
24. Alonso Martínez S, Deco G, Ter Horst GJ, Cabral J. The Dynamics of Functional Brain Networks Associated With Depressive Symptoms in a Nonclinical Sample. Front Neural Circuits. 2020;14:570583.
25. Figueroa CA, Cabral J, Mocking RJT, Rapuano KM, Hartevelt TJ, Deco G, et al. Altered ability to access a clinically relevant control network in patients remitted from major depressive disorder. Hum Brain Mapp. 2019;40:2771–86.
26. Larabi DI, Renken RJ, Cabral J, Marsman J-BC, Aleman A, Ćurčić-Blake B. Trait self-reflectiveness relates to time-varying dynamics of resting state functional connectivity and underlying structural connectomes: Role of the default mode network. NeuroImage 2020;219:116896.
27. Arnold Anteraper S, Triantafyllou C, Sawyer AT, Hofmann SG, Gabrieli JD, Whitfield-Gabrieli S. Hyper-Connectivity of Subcortical Resting-State Networks in Social Anxiety Disorder. Brain Connect. 2014;4:81–90.
28. Chen JE, Lewis LD, Chang C, Tian Q, Fultz NE, Ohringer NA, et al. Resting-state "physiological networks". NeuroImage 2020;213:116707.
29. Johnson FK, Delpech J-C, Thompson GJ, Wei L, Hao J, Herman P, et al. Amygdala hyper-connectivity in a mouse model of unpredictable early life stress. Transl Psychiatry. 2018;8:49.
30. Williams LM. Precision psychiatry: a neural circuit taxonomy for depression and anxiety. Lancet Psychiatry. 2016;3:472–80.
31. Brewin CR, Andrews B, Valentine JD. Meta-analysis of risk factors for posttraumatic stress disorder in trauma-exposed adults. J Consulting Clin Psychol. 2000;68:748–66.
32. Bryant RA. Post-traumatic stress disorder: a state-of-the-art review of evidence and challenges. World Psychiatry. 2019;18:259–69.
33. Melchior M, Caspi A, Milne BJ, Danese A, Poulton R, Moffitt TE. Work stress precipitates depression and anxiety in young, working women and men. Psychol Med. 2007;37:1119–29.
34. Pêgo JM, Sousa JC, Almeida O, Sousa N. Stress and the Neuroendocrinology of Anxiety Disorders. In: Stein MB, Steckler T, editors. Behavioral Neurobiology of Anxiety and Its Treatment, vol. 2, Berlin, Heidelberg:Springer Berlin Heidelberg; 2009. p. 97–118.
35. Hammen C. Stress and Depression. Annu Rev Clin Psychol. 2005;1:293–319.
36. Carvalho AF, Firth J, Vieta E. Bipolar Disorder. N Engl J Med. 2020;383:58–66.
37. Kim EY, Miklowitz DJ, Biuckians A, Mullen K. Life stress and the course of early-onset bipolar disorder. J Affect Disord. 2007;99:37–44.
38. Gispen-de Wied CC. Stress in schizophrenia: an integrative view. Eur J Pharmacol. 2000;405:375–84.
39. Walker E, Mittal V, Tessner K. Stress and the Hypothalamic Pituitary Adrenal Axis in the Developmental Course of Schizophrenia. Annu Rev Clin Psychol. 2008;4:189–216.
40. Avvenuti G, Leo A, Cecchetti L, Franco MF, Travis F, Caramella D, et al. Reductions in perceived stress following Transcendental Meditation practice are associated with increased brain regional connectivity at rest. Brain Cogn. 2020;139:105517.
41. Bergdahl J, Larsson A, Nilsson L-G, Ahlström KR, Nyberg L. Treatment of chronic stress in employees: subjective, cognitive and neural correlates. Scand J Psychol. 2005;46:395–402.
42. Kaul D, Schwab SG, Mechawar N, Matosin N. How stress physically re-shapes the brain: Impact on brain cell shapes, numbers and connections in psychiatric disorders. Neurosci Biobehav Rev. 2021;124:193–215.
43. Taren AA, Gianaros PJ, Greco CM, Lindsay EK, Fairgrieve A, Brown KW, et al. Mindfulness meditation training alters stress-related amygdala resting state functional connectivity: a randomized controlled trial. Soc Cogn Affect Neurosci. 2015;10:1758–68.
44. Caetano I, Amorim L, Soares JM, Ferreira S, Coelho A, Reis J, et al. Amygdala size varies with stress perception. Neurobiol Stress. 2021;14:100334.

45. Hölzel BK, Carmody J, Evans KC, Hoge EA, Dusek JA, Morgan L, et al. Stress reduction correlates with structural changes in the amygdala. Soc Cogn Affect Neurosci. 2010;5:11–7.

46. Archer JA, Lee A, Qiu A, Chen S-HA. Functional connectivity of resting-state, working memory and inhibition networks in perceived stress. Neurobiol Stress. 2018;8:186–201.

47. Jovanovic H, Perski A, Berglund H, Savic I. Chronic stress is linked to 5-HT1A receptor changes and functional disintegration of the limbic networks. Neuroimage 2011;55:1178–88.

48. Lebares CC, Guvva EV, Olaru M, Sugrue LP, Staffaroni AM, Delucchi KL, et al. Efficacy of Mindfulness-Based Cognitive Training in Surgery: Additional Analysis of the Mindful Surgeon Pilot Randomized Clinical Trial. JAMA Netw Open. 2019;2:e194108.

49. Soares JM, Sampaio A, Ferreira LM, Santos NC, Marques P, Marques F, et al. Stress Impact on Resting State Brain Networks. PLoS ONE 2013;8:e66500.

50. Soares JM, Sampaio A, Marques P, Ferreira LM, Santos NC, Marques F, et al. Plasticity of resting state brain networks in recovery from stress. Front Hum Neurosci. 2013;7.

51. Soares JM, Sampaio A, Ferreira LM, Santos NC, Marques F, Palha JA, et al. Stress-induced changes in human decision-making are reversible. Transl Psychiatry. 2012;2:e131.

52. Taren AA, Gianaros PJ, Greco CM, Lindsay EK, Fairgrieve A, Brown KW, et al. Mindfulness Meditation Training and Executive Control Network Resting State Functional Connectivity: A Randomized Controlled Trial. Psychosom Med. 2017;79:674–83.

53. Wu J, Geng X, Shao R, Wong NML, Tao J, Chen L, et al. Neurodevelopmental changes in the relationship between stress perception and prefrontal-amygdala functional circuitry. NeuroImage-Clin. 2018;20:267–74.

54. Esteban O, Markiewicz CJ, Goncalves M, DuPre E, Kent JD, Salo T, et al. fMRIPrep (software). Zenodo; 2021.

55. Esteban O, Markiewicz CJ, Burns C, Goncalves M, Jarecka D, Ziegler E, et al. Nipype (software). Zenodo; 2020.

56. Gorgolewski K, Burns CD, Madison C, Clark D, Halchenko YO, Waskom ML, et al. Nipype: A Flexible, Lightweight and Extensible Neuroimaging Data Processing Framework in Python. Front Neuroinform. 2011;5.

57. Jenkinson M, Beckmann CF, Behrens TEJ, Woolrich MW, Smith SM. FSL. NeuroImage 2012;62:782–90.

58. Smith SM, Jenkinson M, Woolrich MW, Beckmann CF, Behrens TEJ, Johansen-Berg H, et al. Advances in functional and structural MR image analysis and implementation as FSL. NeuroImage 2004;23:S208–S219.

59. Woolrich MW, Jbabdi S, Patenaude B, Chappell M, Makni S, Behrens T, et al. Bayesian analysis of neuroimaging data in FSL. NeuroImage 2009;45:S173–S186.

60. Rolls ET, Joliot M, Tzourio-Mazoyer N. Implementation of a new parcellation of the orbitofrontal cortex in the automated anatomical labeling atlas. NeuroImage 2015;122:1–5.

61. Tzourio-Mazoyer N, Landeau B, Papathanassiou D, Crivello F, Etard O, Delcroix N, et al. Automated Anatomical Labeling of Activations in SPM Using a Macroscopic Anatomical Parcellation of the MNI MRI Single-Subject Brain. NeuroImage 2002;15:273–89.

62. Winkler AM, Ridgway GR, Webster MA, Smith SM, Nichols TE. Permutation inference for the general linear model. NeuroImage 2014;92:381–97.

63. Xia M, Wang J, He Y. BrainNet Viewer: A Network Visualization Tool for Human Brain Connectomics. PLoS ONE. 2013;8:e68910.

64. Vohryzek J, Deco G, Cessac B, Kringelbach ML, Cabral J. Ghost Attractors in Spontaneous Brain Activity: Recurrent Excursions Into Functionally-Relevant BOLD Phase-Locking States. Front Syst Neurosci. 2020;14:20.

65. Lord L-D, Expert P, Atasoy S, Roseman L, Rapuano K, Lambiotte R, et al. Dynamical exploration of the repertoire of brain networks at rest is modulated by psilocybin. NeuroImage 2019;199:127–42.

66. Killgore WDS. Self-Reported Sleep Correlates with Prefrontal-Amygdala Functional Connectivity and Emotional Functioning. Sleep 2013;36:1597–608.

67. Johnstone T, van Reekum CM, Urry HL, Kalin NH, Davidson RJ. Failure to Regulate: Counterproductive Recruitment of Top-Down Prefrontal-Subcortical Circuitry in Major Depression. J Neurosci. 2007;27:8877–84.

68. Cahill L, Uncapher M, Kilpatrick L, Alkire MT, Turner J. Sex-Related Hemispheric Lateralization of Amygdala Function in Emotionally Influenced Memory: an fMRI Investigation. Learn Mem. 2004;11:261–6.

69. Kilpatrick LA, Zald DH, Pardo JV, Cahill LF. Sex-related differences in amygdala functional connectivity during resting conditions. NeuroImage 2006;30:452–61.

70. Cahill L. Sex-Related Influences on the Neurobiology of Emotionally Influenced Memory. Ann N Y Acad Sci. 2006;985:163–73.

71. Cerqueira JJ, Almeida OFX, Sousa N. The stressed prefrontal cortex. Left? Right! Brain Behav Immun. 2008;22:630–8.

72. Clark US, Miller ER, Hegde RR. Experiences of Discrimination Are Associated With Greater Resting Amygdala Activity and Functional Connectivity. Biol Psychiat-Cogn Neurosci Neuroimag. 2018;3:367–78.

73. Banks SJ, Eddy KT, Angstadt M, Nathan PJ, Phan KL. Amygdala–frontal connectivity during emotion regulation. Soc Cogn Affect Neurosci. 2007;2:303–12.

74. Marek S, Dosenbach NUF. The frontoparietal network: function, electrophysiology, and importance of individual precision mapping. Dialogues Clin Neurosci. 2018;20:133–40.

75. Berboth S, Morawetz C. Amygdala-prefrontal connectivity during emotion regulation: a meta-analysis of psychophysiological interactions. Neuropsychologia 2021;153:107767.

76. Cerullo MA, Fleck DE, Eliassen JC, Smith MS, DelBello MP, Adler CM, et al. A longitudinal functional connectivity analysis of the amygdala in bipolar I disorder across mood states: A longitudinal functional connectivity analysis. Bipolar Disord. 2012;14:175–84.

77. Li M, Huang C, Deng W, Ma X, Han Y, Wang Q, et al. Contrasting and convergent patterns of amygdala connectivity in mania and depression: a resting-state study. J Affect Disord. 2015;173:53–58.

78. Magalhães R, Picó-Pérez M, Esteves M, Vieira R, Castanho TC, Amorim L, et al. Habitual coffee drinkers display a distinct pattern of brain functional connectivity. Mol Psychiatry. 2021;26:6589–98.

79. Kolassa I-T, Wienbruch C, Neuner F, Schauer M, Ruf M, Odenwald M, et al. Altered oscillatory brain dynamics after repeated traumatic stress. BMC Psychiatry. 2007;7:56.

80. García-Martínez B, Martínez-Rodrigo A, Fernández-Caballero A, Moncho-Bogani J, Alcaraz R. Nonlinear predictability analysis of brain dynamics for automatic recognition of negative stress. Neural Comput Applic. 2020;32:13221–31.

81. Fontenele AJ, de Vasconcelos NAP, Feliciano T, Aguiar LAA, Soares-Cunha C, Coimbra B, et al. Criticality between Cortical States. Phys Rev Lett. 2019;122:208101.

82. Beggs JM, Timme N. Being Critical of Criticality in the Brain. Front Physio. 2012;3.

ACKNOWLEDGEMENTS

AUTHOR CONTRIBUTIONS
Conceptualization: IC, NS. Methodology: IC, SF, JC, NS. Software: IC, SF, JC. Validation: IC, LA, TCC, CL, MPP, JC. Formal analysis: IC, SF, JC. Investigation: LA, TCC, AC, SF, CPN, JMS, NG, RS, JR, PMarques, PSM, AJR, PM, RM, MPP. Resources: AJR, NCS, PM, NS. Data Curation: AC, RM. Writing - Original Draft: IC. Writing—Review & Editing: JC, NS. Visualization: IC, JC, NS. Supervision: NS. Project administration: NS. Funding acquisition: AJR, NCS, PM, NS.

COMPETING INTERESTS
The authors declare no competing interests.

ADDITIONAL INFORMATION

Supplementary information The online version contains supplementary material available at https://doi.org/10.1038/s41380-022-01780-8.

Correspondence and requests for materials should be addressed to Nuno Sousa.

Reprints and permission information is available at http://www.nature.com/reprints